

Stepwise Behavior of Vortex-Lattice Melting Transition in Tilted Magnetic Fields in Single Crystals of $\text{Bi}_2\text{Sr}_2\text{CaCu}_2\text{O}_{8+\delta}$

J. Mirković,* S. E. Savel'ev,† E. Sugahara, and K. Kadowaki

*Institute of Materials Science, The University of Tsukuba, 1-1-1 Tennodai, Tsukuba 305-8573, Japan
and CREST, Japan Science and Technology Corporation (JST), Japan*

(Received 22 February 2000)

The vortex-lattice melting transition in $\text{Bi}_2\text{Sr}_2\text{CaCu}_2\text{O}_{8+\delta}$ single crystals was studied using in-plane resistivity measurements in magnetic fields tilted away from the c axis to the ab plane. In order to avoid the surface barrier effect which hinders the melting transition in the conventional transport measurements, we used the Corbino geometry of electric contacts. The complete H^c - H^{ab} phase diagram of the melting transition in $\text{Bi}_2\text{Sr}_2\text{CaCu}_2\text{O}_{8+\delta}$ is obtained for the first time. The c -axis melting field component H_{melt}^c exhibits the novel, stepwise dependence on the in-plane magnetic fields H^{ab} which is discussed on the basis of the crossing vortex-lattice structure. The peculiar resistance behavior observed near the ab plane suggests the change of phase transition character from first to second order.

DOI: 10.1103/PhysRevLett.86.886

PACS numbers: 74.60.Ge, 74.60.Ec, 74.72.Hs

In recent years the phase diagram of the vortex state in high temperature superconductors has been reconsidered because the novel vortex phases and phase transitions have been discovered [1]. Among them, the most intriguing phenomenon is the first-order vortex-lattice melting transition (VLMT) [2], the nature of which is not completely understood as of yet. In particular, it is not clear what happens with the melting transition in highly anisotropic systems such as $\text{Bi}_2\text{Sr}_2\text{CaCu}_2\text{O}_{8+\delta}$ if the magnetic field is tilted away from the c axis, especially close to the ab plane, where the second-order phase transition is predicted to occur [3,4].

In contrast to the melting transition in $\text{YBa}_2\text{Cu}_3\text{O}_{7-\delta}$ [5] described well by the anisotropic 3D Ginzburg-Landau (GL) theory [6], it was noticed [7] that VLMT in $\text{Bi}_2\text{Sr}_2\text{CaCu}_2\text{O}_{8+\delta}$ obeys neither 3D GL theory nor 2D scaling [8]. Later, Ooi *et al.* [9] found that the c -axis melting field component H_{melt}^c depends linearly on the in-plane magnetic field H^{ab} in $\text{Bi}_2\text{Sr}_2\text{CaCu}_2\text{O}_{8+\delta}$, which was explained by suppression of Josephson coupling by H^{ab} . On the other hand, Koshelev [10] interpreted the linear dependence of H_{melt}^c on H^{ab} as an indication of the crossing lattice of Josephson vortices (JVs) and pancake vortex stacks (PVSSs). According to this model, the linear dependence $H_{\text{melt}}^c(H^{ab})$ breaks down and transforms into a plateau as soon as the JV cores overlap. Such a plateaulike behavior was observed recently [11,12], but there is still an unresolved question about the underlying mechanisms governing the melting transition in the tilted magnetic fields.

In this Letter, we present a study of the melting transition using the in-plane resistivity measurements in the oblique magnetic fields across the whole angular range. We show that the H^c - H^{ab} phase diagram of the melting transition exhibits a peculiar stepwise behavior, beyond that seen in the existing experimental data or expected in theoretical models. In addition, the change of the phase transition

character from first order to second order is indicated near the ab plane.

The novel experimental findings were obtained essentially by using the Corbino geometry [13] of electric contacts in the resistivity measurements. As is well known, the transport measurements in the conventional four probe strip geometry in $\text{Bi}_2\text{Sr}_2\text{CaCu}_2\text{O}_{8+\delta}$ do not probe the true bulk properties of the superconductor because the surface barriers (related to the Bean-Livingston [14] and geometrical [15] barrier mechanisms) shortcut the current path, and, as a consequence, the currents flow mostly near the sample edges [16]. In order to avoid the effect hindering VLMT by surface barriers, we have used the Corbino electric contact configuration at which currents flow radially, far from the edges of the sample (see the inset in Fig. 1).

The in-plane resistivity measurements were performed for two as-grown single crystals of $\text{Bi}_2\text{Sr}_2\text{CaCu}_2\text{O}_{8+\delta}$ [17] with transition temperature $T_c = 90.3$ K and $T_c = 90.0$ K for samples No. S1 and No. S2, respectively. The diameters of the Corbino disks were $D = 1.9$ mm for No. S1 and 2.7 mm for No. S2, while the thickness was 20 μm for both samples. The resistance was measured by two pairs of electric contacts using the ac lock-in method at a low frequency of 37 Hz, which agree with each other within a geometrical configuration error of about 5%. The measurements of resistance were carried out as a function of the magnetic field H at its different orientation θ with respect to the c axis at various temperatures. The magnetic field was rotated by using a 70 kOe split coil with a fine goniometer having angular resolution of 0.001°.

The magnetic field dependence of the resistance at different orientations measured at a temperature of 85.2 K is shown in Fig. 1. The steep resistance drop attributed to VLMT [18] is clearly detected even in the oblique magnetic fields and, surprisingly, changes quite weakly up to $\theta = 89.86^\circ$. The step height of the resistance anomaly practically remains the same and sharply separates the

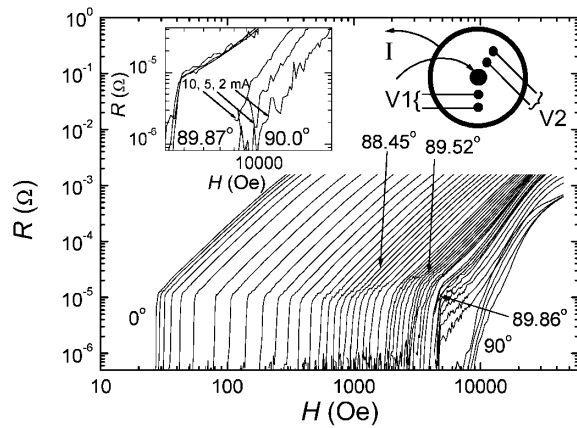


FIG. 1. The magnetic field dependence of the in-plane resistance of $\text{Bi}_2\text{Sr}_2\text{CaCu}_2\text{O}_{8+\delta}$ measured at $T = 85.2$ K at various field orientations with respect to the c axis in sample No. S1 with the current of 5 mA. The arrows labeled with angles 88.45° and 89.52° mark the resistance curves corresponding to the VLMT phase points (Fig. 2) at $H^{ab(1)}$ and $H^{ab(2)}$, respectively. Left inset: The magnetic field dependence of the resistance measured for two field orientations by three current levels. Right inset: A sketch of the sample with the Corbino geometry.

vortex solid and vortex liquid phases. However, as the angle θ exceeds the critical value, only 0.14° away from the ab plane, the resistance level of the kink suddenly begins to decrease, while the sharpness of the anomaly gets even stronger. Surprisingly, an additional 0.1° rotation of the angle from the angle 89.86° causes a dramatic change of the behavior: the kink feature completely vanishes in the instrumental noise and the whole resistance curve shifts to the substantially higher fields, where a qualitatively new, smooth field dependence of $R(H)$ sets in. Instead of the quadratic field dependence, found in the vortex liquid phase, $R(H)$ follows the nonpower law in the extremely narrow angle region $|90^\circ - \theta| < 0.04^\circ$ near the ab plane. It is remarkable that the *Ohmic* response of the resistance observed in the vortex liquid phase at angles $\theta < 89.96^\circ$ is replaced by the *non-Ohmic* behavior (see the inset in Fig. 1).

The vortex dynamics behavior in magnetic fields parallel to the CuO_2 plane looks rather complex. However, the disappearance of the kink anomaly and nonlinear resistance behavior persisting in the high in-plane magnetic fields seems to be induced by the intrinsic pinning [19] due to a periodic variation of the order parameter along the c axis. A suppression of the resistivity kink was observed earlier in the high precision angular measurements for $H \parallel ab$ in $\text{YBa}_2\text{Cu}_3\text{O}_{7-\delta}$ [20], which was associated with the replacement of VLMT by a second-order phase transition in the presence of intrinsic pinning [21]. In this regard, one of the possible physical pictures is that the vortex liquid could condense into the vortex “smectic” phase at a high magnetic field while the smooth vanishing of the resistance may suggest the second-order vortex-crystal–vortex-smectic phase transition [3].

Using the resistance data obtained at two temperatures of 85.2 and 65 K for the sample No. S1, the VLMT phase diagram is constructed in the H^c - H^{ab} plane (Fig. 2). The melting transition was defined by the resistance criterion $R = 10^{-6} \Omega$ over the whole angular range. We should stress that the resistance, in the angular range where the kink exists, does not exhibit the current dependence, the reentrant anomaly, or any other serious indications [22] of the influence of the current distribution through the sample (both along the c axis and inside the Corbino disk) on the detection of the VLMT in our experiments. Moreover, we did not notice any physically meaningful difference between the VLMT determined by the contact pairs V1 or V2 at any field orientations (even very close to the ab plane), which shows that the melting transition does not depend on the mutual orientation of the current and the magnetic field (as we found, the difference between the Corbino geometry and the conventional platelet configurations is only the quality of the data, and the VLMT does not depend on the contact configuration [23]). The in-plane field dependence

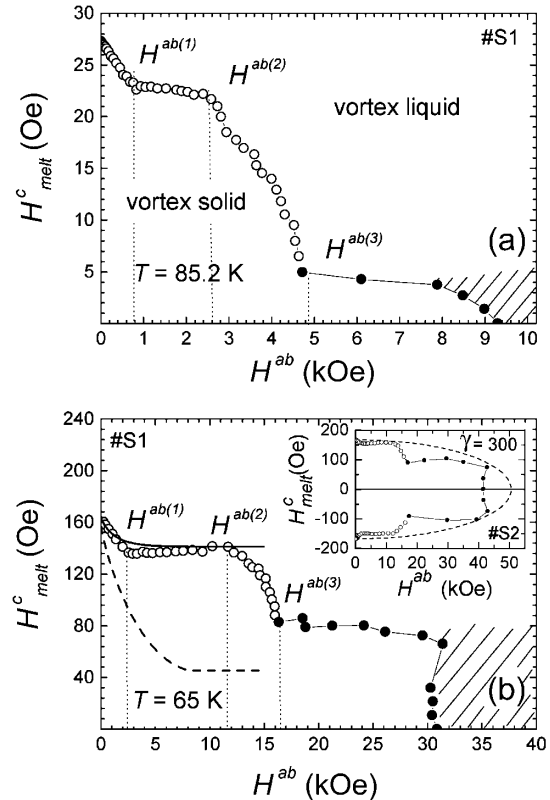


FIG. 2. Vortex-lattice melting transition in the H^c - H^{ab} plane of $\text{Bi}_2\text{Sr}_2\text{CaCu}_2\text{O}_{8+\delta}$ for the sample No. S1 at two different temperatures of 85.2 K (a) and 65 K (b). The dashed line in (b) is the curve obtained from Eq. (8) in [10]. The solid line is the fitted curve after taking into account the crossing lattice pinning. The shaded area marks the region of the nonlinear resistance behavior. Inset in (b): H^c - H^{ab} phase diagram for sample No. S2 at $T = 62$ K. The dashed line corresponds to the anisotropic 3D GL model with the anisotropy parameter of $\gamma = 300$.

of the c -axis melting field component H_{melt}^c exhibits a very intriguing stepwise behavior at both temperatures. In the first stage, H_{melt}^c decreases linearly with the in-plane magnetic field H^{ab} . Then, the linear dependence is abruptly terminated at field $H^{ab(1)}$ and transforms into a plateau which continues to the field $H^{ab(2)}$ where the c -axis component of the melting field H_{melt}^c starts to decrease again. Finally, at the field $H^{ab(3)}$, the so-called “lock-in” transition [24] may occur, while above that field, the phase line (filled symbols in Fig. 2) exhibits a “cusplike” shape and possibly marks the continuous transition to the vortex solid phase. The almost identical H_{melt}^c - H^{ab} phase diagram was obtained in the sample No. S2, as shown in the inset in Fig. 2b at a somewhat lower temperature of 62 K. The obtained H^c - H^{ab} phase diagram of VLMT agrees well with the ac magnetization measurements [12] over the common measured interval $H^{ab} < H^{ab(2)}$. However, in contrast to the ac and dc magnetization technique [7,9,12], the resistance measurements with Corbino geometry do not lose sensitivity even for fields aligned near the ab plane and, thus, make it possible to obtain the complete H_{melt}^c - H^{ab} phase diagram over the whole angular range.

The observed in-plane field dependence of the melting transition is in strong contrast with the 2D scaling [8] ruled only by the out-of-plane magnetic field component. Furthermore, the inset in Fig. 2b demonstrates the essential discrepancy between our data and the fitted curve based on the 3D scaling [6] $H_{\text{melt}}(\theta) = H_{\text{melt}}(0)/(\cos^2\theta + \gamma^{-2}\sin^2\theta)^{1/2}$, where $H_{\text{melt}}(0)$ is the melting field for $\theta = 0^\circ$ and $\gamma = 300$ is chosen as the anisotropy parameter.

The first theoretical examination of the unusual linear dependence $H_{\text{melt}}^c(H^{ab})$ was given by Koshelev [10] who analyzed the crossing vortex lattice with interaction between pancake vortices (PVs) and JVs. Using the general thermodynamic equality of the free energies of vortex solid and vortex liquid phases at the melting transition, Koshelev obtained the linear dependence of the c -axis melting field component: $H_{\text{melt}}^c(H^{ab}) = H_{\text{melt}}^c(0) - 4\pi\epsilon_J H^{ab}/(\Delta B\Phi_0)$, where ϵ_J is the energy of JV in the presence of a PV lattice, ΔB is the jump of the magnetic induction at the melting point, and Φ_0 is the quantum of the magnetic flux [25]. The JV energy ϵ_J , which determines the slope of the linear decay of H_{melt}^c , is calculated in [10] for the case of a dense PV lattice where the size of the JV core $\lambda_J = \gamma s$ exceeds the distance between PVs (Fig. 3a). Figure 2b shows the curve (dashed line) obtained from Eq. (8) of [10] with the same parameters as in that work and a rather high value of the anisotropy $\gamma = 1500$ (the lower values of γ give even stronger discrepancy with experimental data). Although the above mentioned model seems to describe our experimental data qualitatively, the calculated average slope ($dH_{\text{melt}}^c/dH^{ab} \approx 0.025$) as well as the expected breaking field ($H^{ab(1)} = 7$ kOe) appears to be several times higher than our experimental values ($dH_{\text{melt}}^c/dH^{ab} \approx 0.01$,

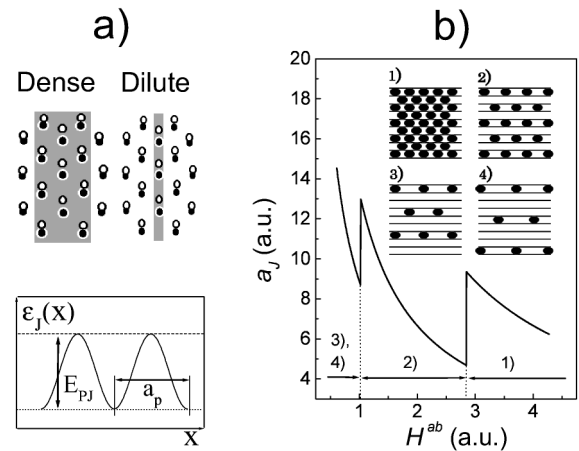


FIG. 3. (a) Top: The schematic picture of the PV lattice deformation due to the interaction with JVs for the dense case $\lambda_J \gg a_p$ and the dilute case $\lambda_J \ll a_p$. The filled circles correspond to PVs in an ideal lattice, while open circles mark PVs in the presence of JV, and the shaded area images the nonlinear JV core. Bottom: The dependence of the JV energy ϵ_J on distance with respect to the dilute PV lattice. (b) The sketch of the in-plane field dependence of the distance a_J between JVs in the same layer. Inset: Possible JV lattices with different periods assuming the discrete occupation of JVs along the c axis.

$H^{ab(1)} \approx 2.5$ kOe). Moreover, in the experimentally studied magnetic field range and for the more realistic value of the anisotropic parameter $\gamma \approx 300$, the size of the nonlinear JV core λ_J is expected to be about the same as the distance between pancake vortices, a_p , which corresponds to the case of the dilute PV lattice (Fig. 3a). In such a case, the energy ϵ_J depends on the relative position of PVS lattice with respect to JV and the minimum of ϵ_J corresponds to the PVS row placed on JV (pinning of PVS by JV [10]). The crossing lattice pinning decreases ϵ_J and, thus, the slope of the linear decay is reduced [26] which improves the correlation between the model and the experimental data (the solid line in Fig. 2b).

Finally, we note that the unusual stepwise behavior of the melting transition seems to be induced by the strong layer structure of $\text{Bi}_2\text{Sr}_2\text{CaCu}_2\text{O}_{8+\delta}$ which governs, in particular, the behavior of the JV lattice. According to Bulaevskii and Clem [27], the JV lattice undergoes sequential structural first-order phase transitions between lattices with different periods (inset in Fig. 3b). These transitions are based on the fact that the JVs are able to occupy only the space in between the CuO_2 planes, i.e., the distance b_J between JVs along the c axis should have discrete values $b_J = ks$, where k is an integer, and s is the distance between CuO_2 planes. The intervortex distance b_J is held constant with the field and sharply reduces only at the structural transitions. On the other hand, the distance a_J between JVs in the same layer decreases as $1/H^{ab}$ and jumps at the transition fields since the magnetic induction should change continuously. As a result, the distance a_J varies nonmonotonously with H^{ab} (Fig. 3b). When a_J is close to a_p , it is reasonable to expect the matching of the

PVS and JV lattices which may activate the crossing lattice pinning responsible for the transformation from linearlike dependence of $H_{\text{melt}}^c(H^{ab})$ to the plateau. Thus, the non-monotonous in-plane field dependence of a_J may induce the second decrease of $H_{\text{melt}}^c(H^{ab})$ as well as the sharp change from one melting regime to another.

In summary, we presented the complete H_{melt}^c - H^{ab} phase diagram of the vortex melting transition in the $\text{Bi}_2\text{Sr}_2\text{CaCu}_2\text{O}_{8+\delta}$ single crystals. In strong contrast to both conventional superconductors and $\text{YBa}_2\text{Cu}_3\text{O}_{7-\delta}$, we observed the stepwise behavior of the melting transition, which reflects the layer structure of the system and may be related to the interaction between pancake vortices and the Josephson vortex lattice. The resistivity behavior indicates that the melting transition may change its character from a first-order to a second-order phase transition in the magnetic fields applied very close to the ab plane.

We appreciate stimulating discussions with A.E. Koshelev, J.R. Clem, W.K. Kwok, M. Tachiki, G. Crabtree, and A.I. Buzdin.

*On leave from Faculty of Sciences, University of Montenegro, P.O. Box 211, 81000 Podgorica, Montenegro, Yugoslavia.

†On leave from All Russian Electrical Engineering Institute, 111250 Moscow, Russia.

- [1] For instance, G. Blatter *et al.*, Rev. Mod. Phys. **66**, 1125 (1994).
- [2] D.R. Nelson and H.S. Seung, Phys. Rev. B **39**, 9153 (1989); E. Zeldov *et al.*, Nature (London) **375**, 373 (1995); A. Schilling *et al.*, Nature (London) **382**, 791 (1996).
- [3] L. Balents and D.R. Nelson, Phys. Rev. B **52**, 12951 (1995).
- [4] X. Hu and M. Tachiki, Phys. Rev. Lett. **80**, 4044 (1998).
- [5] A. Schilling *et al.*, Phys. Rev. B **58**, 11 157 (1998).
- [6] G. Blatter, V.B. Geshkenbein, and A.I. Larkin, Phys. Rev. Lett. **68**, 875 (1992).
- [7] B. Schmidt *et al.*, Phys. Rev. B **55**, R8705 (1997).
- [8] P.H. Kes *et al.*, Phys. Rev. Lett. **64**, 1063 (1990).
- [9] S. Ooi *et al.*, Phys. Rev. Lett. **82**, 4308 (1999).
- [10] A.E. Koshelev, Phys. Rev. Lett. **83**, 187 (1999).
- [11] J. Mirković, E. Sugahara, and K. Kadowaki, Physica (Amsterdam) **284B–288B**, 733 (2000).
- [12] M. Konczykowski *et al.*, Physica (Amsterdam) **341C–348C**, 1213 (2000).
- [13] A. Mazilu *et al.*, Phys. Rev. B **58**, R8913 (1998).
- [14] C.P. Bean and J.D. Livingston, Phys. Rev. Lett. **12**, 14 (1964).
- [15] E. Zeldov *et al.*, Phys. Rev. Lett. **73**, 1428 (1994).
- [16] D.T. Fuchs *et al.*, Nature (London) **391**, 373 (1998).
- [17] T. Mochiku and K. Kadowaki, Trans. Mater. Res. Soc. Jpn. **19A**, 349 (1993).
- [18] S. Watauchi *et al.*, Phys. **C259**, 373 (1996); J. Mirković, K. Kimura, and K. Kadowaki, Phys. Rev. Lett. **82**, 2374 (1999).
- [19] M. Tachiki and S. Takahashi, Solid State Commun. **70**, 291 (1989).
- [20] W.K. Kwok *et al.*, Phys. Rev. Lett. **73**, 2614 (1994).
- [21] However, the proposed scenario has not been confirmed by thermodynamic measurements yet [Ref. [5], see also T. Ishida *et al.*, Phys. Rev. B **58**, 5222 (1998)].
- [22] B. Khaykovich *et al.*, Phys. Rev. B **61**, R9261 (2000).
- [23] The possible problems arising sometimes from the Corbino geometry [G. D'Anna *et al.*, Phys. Rev. B **54**, 6583 (1996)] are of no importance in our measurements.
- [24] D. Feinberg and C. Villard, Phys. Rev. Lett. **65**, 919 (1990); A.E. Koshelev, Phys. Rev. B **48**, 1180 (1993).
- [25] This result can easily be derived from the general thermodynamic equation at the melting transition: $F_s^c(B_{m0}^c + \delta B_m^c) + \delta F_s = F_l^c(B_{m0}^c + \delta B_m^c) + \delta F_l$, where F_s^c and F_l^c are the free energies of the vortex solid and the vortex liquid states for the c -axis magnetic field, respectively, B_{m0}^c is the melting field in $H^{ab} = 0$, δB_m^c is the shift of the c -axis melting field induced by H^{ab} , while δF_s and δF_l are the contributions to the free energies born by the in-plane magnetic field. Expanding F_s^c and F_l^c with respect to δB_m^c as $F_s^c(B_{m0}^c + \delta B_m^c) - F_l^c(B_{m0}^c + \delta B_m^c) = (\partial F_s^c / \partial B_{m0}^c - \partial F_l^c / \partial B_{m0}^c) \delta B_m^c = \Delta M \delta B_m^c$, one gets $B_m^c = B_{m0}^c - 4\pi(\delta F_s - \delta F_l) / \Delta B$. In the case of a crossing lattice, $\delta F_s = (B^{ab})^2 / 8\pi - \epsilon_J B^{ab} / \Phi_0$, i.e., it consists of the magnetic energy and the energy of JVs in the presence of PV lattice. Taking into account that the Josephson coupling is suppressed in the vortex liquid state [$\delta F_l \approx (B^{ab})^2 / 8\pi$] and neglecting the difference between magnetic induction and external magnetic field, we obtain the equation as presented in the text.
- [26] The pinning energy E_{PJ} (Fig. 3a) can be evaluated as a difference of the energy of a PVS row placed on JV and the energy of a PVS row shifted on the distance $a_p/2$ from JV. The corresponding contribution to the slope $dH_{\text{melt}}^c/dH^{ab}$ is $4\pi A E_{\times} a^p / (\Phi_0 \lambda_J^2 \Delta B)$, where E_{\times} is the energy of a single PVS on JV defined by Eq. (9) in [10] and A is about unity.
- [27] L. Bulaevskii and J.R. Clem, Phys. Rev. B **44**, 10234 (1991).